Key Mechanistic Features of a Silver(I)-Mediated Deconstructive Fluorination of Cyclic Amines: Multi-State Reactivity versus Single Electron Transfer

Jose B. Roque^{||}, Richmond Sarpong*, and Djamaladdin G. Musaev*, and Djamaladdin G. Musaev*,

ABSTRACT: Density functional calculations have provided evidence that a Ag(I)-mediated deconstructive fluorination of *N*-benzoylated cyclic amines (**LH**) with Selectfluor® [(F–TEDA)(BF₄)₂] begins with an association of the reactants to form a singlet state adduct {[(**LH**)-Ag]-[F-TEDA]²⁺}. The subsequent formation of an iminium-ion intermediate, [**L***-Ag]–HF–[TEDA]*, is, formally, a Ag(I)-mediated hydride abstraction event that occurs in two steps: (a) a formal oxidative addition (*OA*) of [F-TEDA]²⁺ to the Ag(I)-center that is attended by an electron transfer (*ET*) from substrate (**LH**) to the Ag-center (i.e., *OA+ET*, this process can also be referred to as a F-atom coupled electron transfer), followed by (b) H-atom abstraction from **LH** by the Ag-coordinated F-atom. The overall process involves lower-lying singlet and triplet electronic states of several intermediates. Therefore, we, formally, refer to this reaction as a *two-state reactivity* (*TSR*) event. The C–C bond cleavage/fluorination of the resulting hemiaminal intermediate via a ring-opening pathway has also been determined to be a *TSR event*. A competing deformylative fluorination initiated by a hemiaminal to aldehyde equilibration involving formyl H-atom abstraction by a TEDA²⁺ radical dication, decarbonylation, and fluorination of the resulting alkyl radical by another equivalent of Selectfluor® may also be operative in the latter step.

INTRODUCTION

The functionalization of "inert" C-H bonds by converting them to C-C or C-X bonds (where X is a heteroatom such as O, N, B, etc.) has revolutionized the synthesis and production of pharmaceuticals, agrochemicals, materials and fuels.^{1,2} Similarly, the utilization of C-C and C-X bonds to form new bonds by cleavage and functionalization of their constituent groups may lead to products which cannot be prepared efficiently by other means (i.e., these products possess high synthetic complexity).3-7 In particular, the development of methodologies for the deconstructive functionalization of cyclic amines (i.e., scaffold cleavage/functionalization) may provide new opportunities for diversifying these structural motifs that are abundant in pharmaceuticals and agrochemicals. Among the many deconstructive strategies that have been developed is a method by Sarpong and coworkers that is proposed to proceed through a distinct mechanism.^{8,9} This method transforms N-acylated saturated aza-cycles (e.g., 1, Scheme 1) into versatile fluorinecontaining acyclic amine derivatives (e.g., 3) using the commercially available reagents Selectfluor® (2) and AgBF₄. Presumably, the transformation occurs through a selective C(sp³)-C(sp³) bond cleavage in the presence of a C(sp³)-N bond. An indepth understanding of the mechanism of this unusual transformation should (a) facilitate the development of a more general strategy for the deconstructive functionalization of cyclic amines, and (b) enable the identification of alternative

oxidizing salts and fluorinating reagents that are less expensive, and may improve the functional group compatibility of the process.

Scheme 1. Silver-Mediated Deconstructive Fluorination of *N*-Benzoylated Cyclic Amine 1.

Sarpong and coworkers proposed a two-stage mechanism, each mediated by a silver salt and Selectfluor®, for the transformation of $\mathbf{1} \to \mathbf{3}$ (Figure 1).^{8,9} In the first stage, cyclic amine $\mathbf{1}$ is oxidized by the combination of AgBF₄ and Selectfluor® to the corresponding iminium ion (\mathbf{A}), which is trapped by H₂O to form hemiaminal \mathbf{B} (Figure 1d). Selectfluor® and AgBF₄ did not react in the absence of substrate, indicating the importance of Ag(I) binding to the amide moiety of $\mathbf{1}$ to reactivity. In line with previous studies, ¹⁰⁻²⁶ as well as their own mechanistic analysis, Sarpong and co-workers proposed that the Ag(I)-center binds to $\mathbf{1}$ to form adduct $\mathbf{4}$ (Figure 1A). Upon interaction of this adduct with $\mathbf{2}$, a single electron transfer occurs from the ligated AgBF₄ of $\mathbf{4}$ to $\mathbf{2}$ to generate a Ag(II)-center and radical dication $\mathbf{5}$. The resulting Ag(II) then oxidizes an equivalent of $\mathbf{1}$ through single-electron transfer (SET)²⁷ and

[#] Cherry L. Emerson Center for Scientific Computation, and Department of Chemistry, Emory University, Atlanta, GA 30322.

¹¹ Department of Chemistry, University of California, Berkeley, CA 94720

subsequent hydrogen-atom abstraction by 5 delivers iminium ion **A** (Figures 1A and 1B). An alternative pathway, where radical dication 5 effects α -amino C–H abstraction from 1 to generate an α -amino radical (E) followed by single-electron transfer to Ag(II) to generate **A**, was also proposed (Figure 1C). In the next stage, iminium ion **A** is trapped by H₂O to give hemiaminal **B** (Figure 1D).

In the second stage of the reaction, the resulting hemiaminal (B) is transformed to the final products (3 or 9; Figures 1E and F). This stage of the overall transformation was proposed to proceed through two possible pathways. In Path-A (Figure 1E), hemiaminal B reacts with Ag(I) and 2 to form radical C. Presumably, a deprotonation of the hemiaminal and single electron transfer generates an alkoxy radical intermediate that is homolyzed through selective C(sp³)-C(sp³) bond cleavage to give C.3 A radical fluorination of C by 2 then forms alkyl fluoride product 3. Alternatively, Path-B (Figure 1F), referred to by Sarpong and coworkers as the 'deformylation pathway' in their initial communications, would involve (a) heterolytic C-N bond cleavage of hemiaminal B to linear aldehyde 7 and subsequent oxidation of the formyl group to the corresponding carboxylic acid (8), and finally (b) decarboxylative fluorination to afford 9.8,9

Even though the proposed mechanistic scenarios in Figure 1 are consistent with those previously described for ring-opening functionalization and transition metal catalyzed fluorination methods, 10-26 the elementary steps, relevant intermediates, and transition states remained to be fully elucidated. We viewed this fundamental knowledge to be vital to identifying simpler, more efficient protocols for the deconstructive fluorination of *N*-acylated cyclic amines. Therefore, the aims of the computational studies reported here are to provide insight into the mechanism of the Ag(I)-mediated deconstructive fluorination of *N*-acylated cyclic amine 1 with Selectfuor®.

The calculations presented herein, consistent with previous proposals, ^{8,9} show that formation of iminium ion **A** from **1**, in the presence of AgBF₄ and Selectfluor® (**2**) is, formally, a Ag(I)-mediated hydride abstraction event. We have established, for the first time, that this occurs through: (a) a formal oxidative addition (*OA*) of [F-TEDA]²⁺ to the Ag(I)-center that is attended by an electron transfer (*ET*) from substrate (**LH**) to the Ag-center (i.e., *OA+ET*, this process can also be referred to as a F-atom coupled electron transfer, FCET), followed by (b) abstraction of an H-atom from the radical cation of **1** by the Ag-bound F-atom. This reaction involves low-lying singlet and triplet electronic states of the reactive intermediates, and, therefore, is characterized as a *two-state reactivity (TSR)* process, ²⁸⁻³⁵ rather than a classical *single-electron-transfer (SET)* event.

We have shown that the subsequent fluorination of the resulting hemiaminal (\mathbf{B}) via the ring-opening mechanism (Path A, Figure 1E) begins with a H-atom abstraction from the hydroxy group, and is also a TSR event. However, the alternative "deformylative" fluorination pathway (i.e., $\mathbf{7} \rightarrow \mathbf{9}$), that may be initiated by equilibration of the hemiaminal to aldehyde, followed by its oxidation to a carboxylic acid and subsequent decarboxylative fluorination or, alternatively, H-atom abstraction from $\mathbf{7}$ by $\mathbf{5}$, decarbonylation, and fluorination by another

equivalent of Selectfluor®, is not a *TSR* event. Both net C–C cleavage/fluorination pathways (i.e., Path A and Path B) are feasible. The operative pathway likely depends on the reaction conditions, and the electronic properties of the *N*-acyl group in **1**.

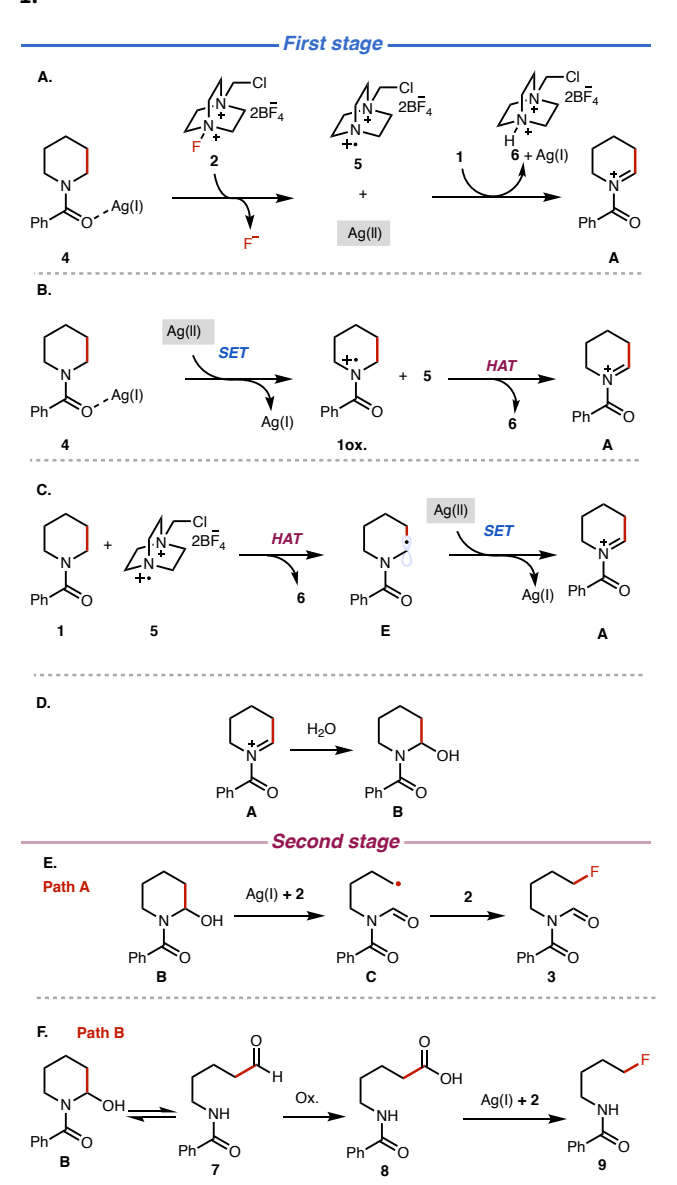


Figure 1. Proposed mechanisms for the deconstructive fluorination: (A) Overall oxidation sequence, (B) single electron transfer (SET) occurs first, (C) hydrogen atom transfer (HAT) occurs first, (D) hemiaminal **B** formation from iminium ion **A**, (E) homolytic C—C cleavage, Path A, and (F) heterolytic C—N cleavage, Path B.

Experimental: Computational Details

All reported structures were calculated using the Gaussian-16 suite of programs³⁶ at the B3LYP-D3(BJ)/[6-31G(d,p) + Lanl2dz (Ag)] level of theory with the corresponding Hay-Wadt effective core potential³⁷⁻³⁹ for Ag. Here we used the B3LYP density functional⁴⁰⁻⁴² with Grimme's empirical dispersion-correction (D3)⁴³ and Becke-Johnson (BJ) damping-correction.⁴⁴⁻⁴⁶ Frequency analyses were used to characterize each minimum with

zero imaginary frequency and each transition state (TS) structure with one imaginary frequency. Intrinsic reaction coordinate (IRC) calculations were performed for all TSs to ensure their true nature. Bulk solvent effects were incorporated for all calculations (including geometry optimizations and frequency calculations) using the self-consistent reaction field polarizable continuum model (IEF-PCM). 47,48 We chose water as solvent. The reported thermodynamic data were computed at a temperature of 298.15K and at 1atm of pressure. Various lower lying electronic states, including the open-shell singlet states (where appropriate) were considered for all key species. Unless otherwise stated, energies are given as $\Delta H/\Delta G$ in kcal/mol.

The open-shell singlet states of $\mathbf{5c}$ and $\mathbf{10c}$ are only slightly higher in free energy as compared to the corresponding triplet states, which enabled us to characterize the $\mathbf{5c-s} \to \mathbf{5c-t}$ and $\mathbf{10c-s} \to \mathbf{10c-t}$ transitions as two state reactivity events. Since these small energy values are subject to the level of theory employed, adiabatic transitions (i.e., singlet state-to-singlet state transitions involving high- and low-spin states) cannot be ruled out. A search for transition states associated with adiabatic transitions requires multi-determinant approaches which are not practical for such large chemical systems. Triplet states were determined to be more in line with our analyses and allow consistency in our presentation of the major chemical outcomes of this study.

Following an extensive computational survey, we employ dication (F-TEDA)²⁺, without the two corresponding BF₄-counter anions, as a model for Selectfluor® (see Figure S1 in the Supporting Information for details). Below we use "**Xc-y**" labeling to denote calculated structures, where **X** is a number associated with a structure and **c** denotes computed. The label **y** indicates singlet (**s**), doublet (**d**), and/or triplet (**t**) states.

In order to validate the [B3LYP-D3(BJ)+PCM]/[6-31G(d,p) + Lanl2dz (Ag)] approach in this study, we have performed a series of calculations at the highest possible levels of theory for critical points along the computed potential energy surfaces. Specifically, the formation of [(LH)-AgBF₄] from LH and AgBF₄, $\Delta H_{comp}/\Delta G_{comp}$, and the singlet-triplet energy splitting [i.e., E(S– T)] in complexes 5c and 10c (see below) were re-calculated at the [B3LYP-D3(BJ)+PCM]/[cc-pVTZ + Lanl2dz(f) (Ag)]⁴⁹ level of theory (to validate the [6-31G(d,p) + Lanl2dz (Ag)] basis sets that we employed), and at the [wB97XD+PCM]/[cc-pVTZ + Lanl2dz(f) (Ag)]50 level of theory (to validate the use of B3LYP density functional). Results of these calculations are given in the Supporting Information (see Table S1). We found that changing the basis sets from [6-31G(d,p) + Lanl2dz(Ag)] to [ccpVTZ + Lanl2dz(f)(Ag)] reduced the calculated complexation free energy, and the E(S-T) of complexes 5c and 10c by ~1-2 kcal/mol. In addition, we found that the choice of the density functional strongly impacts several calculated properties. For example, upon going from [B3LYP-D3(BJ)] to wB97XD functionals, the complexation free energy decreased by 3.4 kcal/mol, and the E(S-T) increased by 1.0 and 6.8 kcal/mol, for complexes 5c and 10c, respectively. Importantly, neither using larger basis sets, or the wB97XD functional (instead of [B3LYP-D3(BJ)]) altered our conclusions.

A. Mechanism of the Iminium-ion formation. Consistent with previous^{8,9} experimental findings, our calculations show that AgBF₄ (denoted as Ag(I), below) binds the substrate (LH, Figure 2) to form adduct [(LH)–Ag(I)], 4c. For the ground singlet electronic state of this complex, i.e., 4c-s, the calculated interaction between LH and Ag(I) (favorable by 20.5/8.9 kcal/mol) results in a slight elongation of the carbonyl C–O bond (from 1.238 to 1.264 Å), and a shortening of the N–carbonyl bond (from 1.361 to 1.341 Å).⁵² A charge density analysis indicates that in 4c-s, a 0.20 |e| charge is transferred from LH to Ag(I) (for more details, see Figure S2 in the Supporting Information).

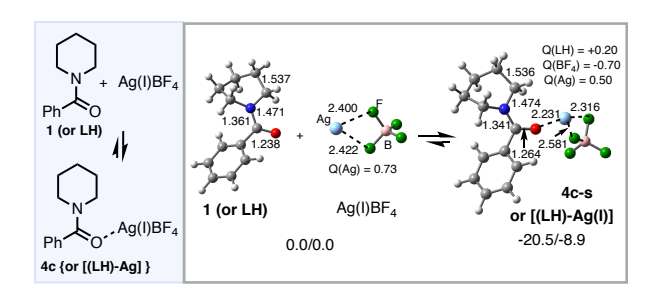


Figure 2. Selected structural and electronic parameters (distances are in Å and Mulliken charges, Q, are in |e|). Relative energies ($\Delta H/\Delta G$ in kcal/mol) are indicated for **LH** (or **1**), AgBF₄, and singlet state adduct (**LH**)[AgBF₄], **4c-s**.

Interaction of **4c-s** with (F-TEDA)²⁺ leads to complex **5c-s**. As seen in Figure 3, the geometry and charge distributions in the [(**LH**)-Ag] and (F-TEDA)²⁺ fragments did not change noticeably upon interaction of (F-TEDA)²⁺ and [(**LH**)-Ag]. In complex **5c-s** (Figure 3), a charge of almost +2 is located on (F-TEDA), and only an additional 0.12 |e| electron is distributed from **LH** to the AgBF₄-unit.

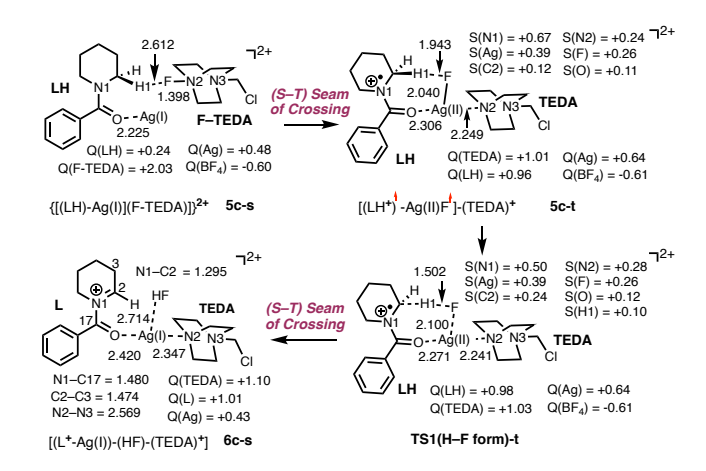


Figure 3. Calculated intermediates **5c-s**, **5c-t**, and **6c-s**, and triplet transition state **TS1** (**H–F form)-t** along with their important geometry (distances are in Å) and electronic parameters (Mulliken charges, **Q**, and spin densities, **S**, are in |e|). For simplicity, BF₄-anion and non-interacting H atoms are omitted. For details, see Figure S3 in the Supporting Information.

Calculations show that the generation of iminium 6c-s from complex 5c-s is highly unfavorable on the singlet energy surface (see below). However, reasonable energies were computed for the reaction proceeding via a singlet-triplet seam of crossing. Here, we were not able to locate/optimize the minimum of the seam of crossing (MSX) for such large and conformationally unrestrained systems.⁵² However, triplet state intermediate 5c-t is only 13.4/13.5 kcal/mol higher in energy than **5c-s** (see also Figure 4). As seen in Figure 3, the **5c-s** \rightarrow **5c**t transition results in the cleavage of the F-TEDA bond, and formation of the Ag-F (bond distance = 2.040Å) and Ag-TEDA (Ag-N2 = 2.246 Å) bonds. Furthermore, in **5c-t**, the **LH**fragment has 0.96 |e| positive charge and 1.11 |e| unpaired α -spin (i.e., it is a radical cation similar to **10x** in Figure 1), and another unpaired α -spin is delocalized on AgF (as 0.39 |e| and 0.26 |e| spins on Ag and F, respectively) and a mono-cationic TEDA⁺ fragment that is coordinated to Ag.⁵³ The Ag-center has also lost electron density compared to that in 5c-s: it now bears a +0.68 |e| positive charge and a 0.39 |e| unpaired α -spin. Thus, the Ag-center is further oxidized in 5c-t. The computed charge, spin distributions, and geometry parameters enabled us to characterize 5c-t as a Ag(II) species with a weak Ag-F interaction [(LH $^+$) $^-$ -(AgF $^-$) – (TEDA) $^+$], and the 5c-s \rightarrow 5c-t transi-

tion as a fluorine atom coupled electron transfer (FCET)

process. Formally, the $5c-s \rightarrow 5c-t$ transition can also be viewed as an oxidative addition (OA) of F–TEDA to Ag(I) coupled with an electron transfer (ET) from **LH** (an OA+ET). However, the exact nature of this dynamic process (synchronous versus asynchronous) remains undetermined.

Historically, Ag(I) has been implicated in mainly one-electron redox chemistry. Therefore, we propose that the formal oxidative addition involves multiple steps (*vide infra*). However, the exact nature of this dynamic process remains to be determined since we only observe rapid electron transfer from **LH**. Reports proposing Ag(III)—F species have remained unsubstantiated. However, recently, Ribas and co-workers have reported the synthesis of well-defined Ag(III)-aryl complexes generated from a Ag(I)/Ag(III) redox cycle.⁵⁴ Furthermore, recently, Musaev and coworkers have identified a critical Ag(III)-intermediate in the Cu-catalyzed, Ag-salt mediated, Ullmanntype coupling reaction. ⁵⁵

Since, (a) we were not able to locate transition states for the Ag(I) oxidative addition to F–TEDA (neither on the singlet nor triplet state PESs), and (b) the $\mathbf{5c-s} \to \mathbf{5c-t}$ transition involves lower-lying singlet and triplet states of the initial $\mathbf{5c-s}$ and product $\mathbf{5c-t}$ complexes, here, we describe the $\mathbf{4c-s} + [F-TEDA]^{2+} \to \mathbf{5c-s} \to \mathbf{5c-t}$ transformation as a two-state reactivity (TSR) event. ²⁸⁻³⁵

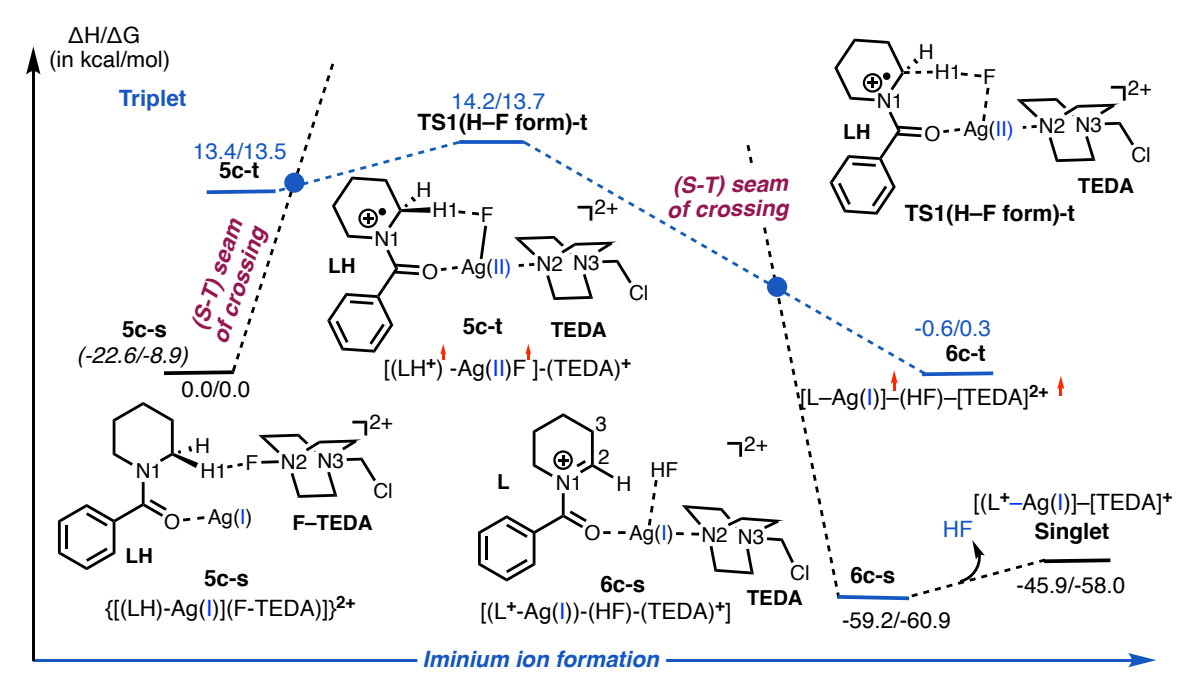


Figure 4. Schematic representation of the calculated energy profile for iminium-ion formation upon interaction of *N*-protected cyclic amine **LH**, AgBF₄-catalyst, and Selectfluor[®]. Energies are provided relative to the intermediate **5c-s**. Energies given in parentheses are relative to the dissociation limit of [(**LH**)–Ag(I)], **4c**-s, + 2[F-TEDA]²⁺.

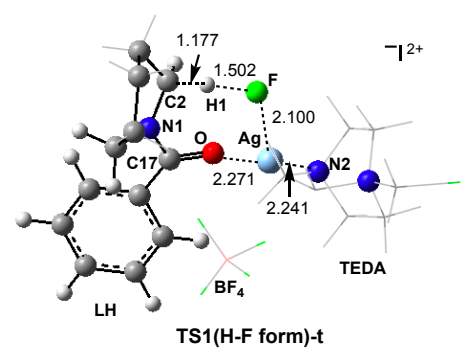
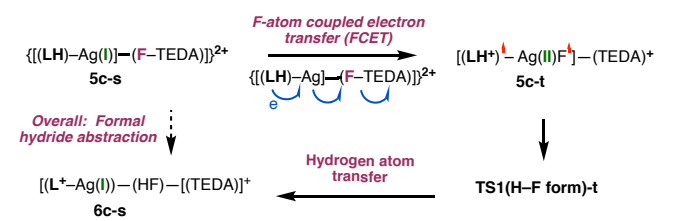


Figure 5. Computed triplet transition state TS1(H-F form)-t for H–F formation that connects intermediates 5c-t and 6c-t (distances are in Å).

From 5c-t, H-F bond formation leads to iminium ion 6c {[L-Ag]-(HF)-[TEDA]}²⁺, the ground electronic state of which is the singlet state: complex 6c-s lies 59.2/60.9 kcal/mol lower in energy than pre-reaction complex 5c-s. The triplet state of 6c, i.e., 6ct, lies 58.6/61.2 kcal/mol higher in energy than 6c-s (see Figure S3 in the Supporting Information). Rigid scanning of the singlet potential energy surface for the HF-formation indicated that the singlet transition state [TS1(H-F form)-s] that may directly connect 5c-s with 6c-s lies very high in energy (see dotted black line in Figure 4). Therefore, a search for TS1(H-F form)-s was not pursued. Gratifyingly, we were able to locate the triplet transition state, TS1(H-F form)-t, that directly connects 5c-t with 6c-t (see Figure 5). Our analyses show that TS1(H-F form)t is a H-atom abstraction transition state from LH by the Agcoordinated F-atom.⁵⁶ The reactivity of amidyl radical cation **5c-t** is consistent with observations from prior studies wherein an amine participates in a hydrogen atom transfer event upon single electron oxidation. 57 Notably, the α -C-H bond of amine is estimated to be significantly weakened (lower BDE) following single electron oxidation.⁵⁷ In the resulting product complex 6c-s, where an HF molecule is formed, the [L+-Ag] fragment possesses only one positive charge, which is mostly located on the now oxidized piperidine ring of L. As illustrated in Figure 4, TS1(H-F form)-t lies higher (by 0.8/0.2 kcal/mol) relative to triplet state complex 5c-t, and is not expected to be traversed in the productive reaction path.

Scheme 2. Proposed *Two-State Reactivity* Mechanism for 6c-s Formation From *N*-Benzoylated Cyclic Amine LH, Ag(I)-Salt, and [F-TEDA]²⁺.



The formation of the iminium ion is summarized in Scheme 2 from **5c-s** and involves: (a) F-atom transfer from [F-TEDA]²⁺ to the Ag-center of the adduct [(**LH**)-Ag] which is coupled with an electron transfer from the substrate (**LH**) to the AgF-fragment [a fluorine atom coupled electron transfer (FCET); formally, a Ag(I) oxidative addition to N–F coupled with

an electron transfer, i.e., OA+ET)], triggered by a singlet-to-triplet (S-T) transition to arrive at **6c-t**, followed by (b) H-atom abstraction from **LH** by the Ag-coordinated F-atom. Since this reaction involves lower-lying singlet and triplet electronic states of the reactive intermediates, we characterize it as a two-state reactivity (TSR) process. ²⁸⁻³⁵

A plausible alternative mechanism consistent with literature precedent (predominantly in oxidative photoredox, as well as in first-row transition metal catalysis) may also be operative. 15,18,25 This may begin by single electron transfer from Ag(I) to Selectfluor® to form an aminium dication radical TEDA2+, Ag(II), and fluoride ion. H-atom abstraction of the α -C-H bond of the substrate (**LH**) by the aminium radical dication TEDA2+, forms α -amino radical, which can undergo further oxidation to generate an iminium ion. Our calculations show that this process is highly unfavorable (by 36.4/35.0 kcal/mol). Since both our calculations and our empirical observations 8,9 indicate that **LH** and Ag(I)-salt form an adduct [(**LH**)-Ag(I)] i.e., **4c-s**, we also studied thermodynamics of the reaction

$$[(LH)-Ag(I)] + [F-TEDA]^{2+} \rightarrow [(LH)-Ag(II)-F] + TEDA^{2+}$$

and found that this reaction is endergonic (by 27.8/26.4 kcal/mol). Furthermore, coordination of the TEDA²⁺ radical to [(LH)-Ag(II)-F] to form the triplet state complex **5c-t**, discussed above, is exergonic by 14.3/25.7 kcal/mol. Our computational data has, therefore, enabled us to rule out this alternative mechanism which resembles the pathway depicted in Figure 1C. These data support a formal oxidative addition of Ag(I) to F-TEDA which proceeds in a step-wise fashion (*vide supra*).

Mechanism for the conversion of iminium ion complex 6c-s to hemiaminal complex 8c-s. Even though the mechanism for hemiaminal formation was anticipated to be straightforward, we have nonetheless computed energies and structures of the relevant intermediates and products for completeness of the discussion. In this regard, iminium ion complex 6c-s, [(L+-Ag)–(HF)–(TEDA) $^+$], undergoes HF \rightarrow H₂O exchange to form $[(L^+-Ag)-(H_2O)-(TEDA)^+]$ (7c-s, Figure 6). This process requires 13.3/2.9 kcal/mol energy for the HF dissociation (see Figure 4), and is exergonic by 11.6/12.0 kcal/mol. In 7c-s, the (L+-Ag)fragment bears one positive charge, and another positive charge is delocalized on the [TEDA]+ fragment. The deprotonation of the Ag-bound water by the TEDA, and the subsequent C2-OH bond formation is expected to be a facile process. Here, we were not able to locate the transition state associated with the conversion of 7c-s to 8c-s, [(LOH)-Ag](H-TEDA)²⁺. Calculations show that the overall process for the conversion of iminium ion complex 6c-s to hemiaminal complex 8c-s is exergonic by 10.0/8.3 kcal/mol.

Close examination of the calculated Mulliken charges supports the characterization of **8c-s** as a [(**LOH**)-Ag(I)](H-TEDA)²⁺ complex (see Figure 6).⁵⁸

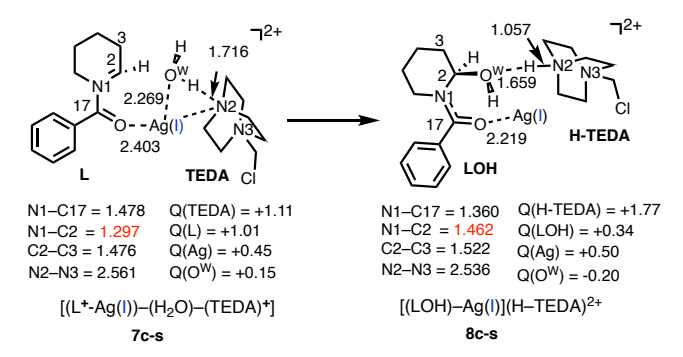


Figure 6. Calculated iminium-ion and hemiaminal complexes **7c-s** and **8c-s**, along with their important geometry and electronic parameters (distances are in Å, and Mulliken charges, **Q**, are in |e|)). For more details, see Figure S4 in the Supporting Information.

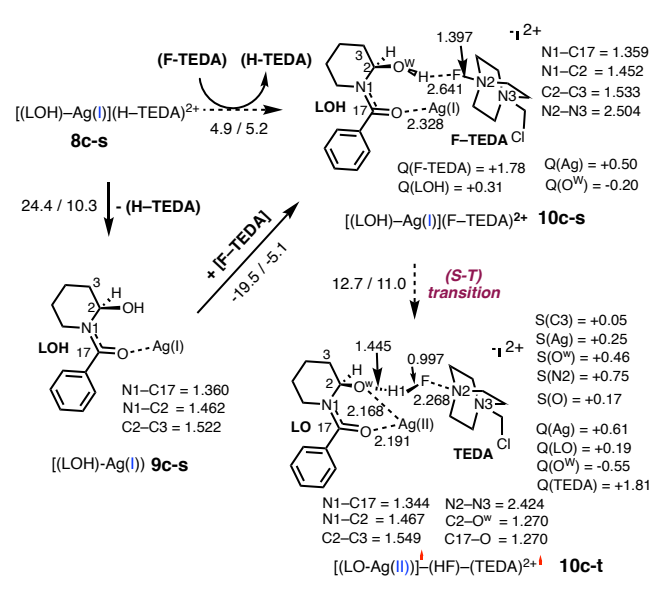


Figure 7. Computed structures for **9c-s, 10c-s,** and **10c-t,** along with their geometry and electronic parameters (distances are in Å, Mulliken charges, Q, and spin densities, S, are in |e|). Energies of each step of the reaction are provided as $\Delta H/\Delta G$ in kcal/mol. For more details, see Figure S5 in the Supporting Information.

C. Fluorination of hemiaminal complex 8c-s. As illustrated in Figure 1, hemiaminal **B** (i.e., **LOH** in Figures 6 and 7) can be converted to the final fluorinated products via two competing pathways: homolytic β -C–C cleavage (Path-A, Figure 1E) or loss of the aldehyde group (by oxidation to the carboxylic acid and decarboxylation; Path-B, Figure 1F).

C.1. Homolytic C–C cleavage pathway (Path A). Path-A is proposed to be initiated by an $(H-TEDA)^{2+} \rightarrow (F-TEDA)^{2+}$ exchange that converts hemiaminal complex **8c-s** to intermediate **10c-s** (i.e., [(LOH)-Ag](F–TEDA)^{2+}, (see Figures 7 and 8). This process is endergonic by 5.2 kcal/mol, and may proceed via either the dissociation of $(H-TEDA)^{2+}$ and coordination of $(F-TEDA)^{2+}$ (i.e., a stepwise) or a concerted $(H-TEDA)^{2+} \rightarrow (F-TEDA)^{2+}$ exchange pathway. Calculations show that the stepwise pathway requires 10.3 kcal/mol free energy for dissociation of $(H-TEDA)^{2+}$. This energy value can also be taken as an upper limit for the

concerted (H-TEDA) $^{2+}$ \rightarrow (F-TEDA) $^{2+}$ exchange. Thus, the free energy required for **8c-s** \rightarrow **10c-s** (at a maximum of 10.3 kcal/mol) is unlikely to impact the overall outcome of the reaction.

Ring-opening from 10c-s could, in principle, proceed through either direct H-F bond formation on the singlet state energy surface or a two-state reactivity (TSR) mechanism initiated by a singlet-to-triplet seam of crossing, i.e., via the (S-T) transition. Our studies indicate that HF formation in 10c-s via a TSR mechanism is more favorable and requires about 11.0-12.0 kcal/mol of free energy (see Figures 7 and 8). As depicted in Figure 7, the transition from 10c-s to 10c-t results in not only a ground electronic state change, but also significant geometry alterations: in 10c-t, the Ow-H and N2-F bonds are significantly elongated, and the H-F bond (0.997 Å) and the Ag-Ow bond (2.168 Å) are almost fully formed. Spin, charge density, and geometry analyses of **10c-t** show that the **10c-s** \rightarrow **10c-t** transition leads to simultaneous F-atom and H-atom coupling to form HF, and dicationic TEDA²⁺ and [(LO)-Ag] radicals. In the TEDA²⁺ radical, a 0.75 |e| unpaired electron is located on the proximal N2-center. Importantly, in the [(LO)-Ag] fragment, the Ag-center has acquired more positive charge (compared to that in **10c-s**) and bears 0.25 [e] unpaired α -spin. These findings are indicative of the Ag being partly oxidized in complex **10c-t**. On the basis of these analyses, we characterize **10c-t** as a diradical intermediate [(LO)-Ag(II)]*-(HF)-(TEDA)^{2+*}.

In the next stage, intermediate $\mathbf{10c\text{-}t}$ is converted to alkoxide complex $\mathbf{11c}$, $\{[(\mathbf{LO})\text{-}Ag]\text{-}(FH)\text{-}(TEDA)\}^{2+}$ featuring a hydrogen and TEDA interaction. This transition is expected to be a facile process since it mostly involves breaking and formation of weak O--HF and FH--TEDA hydrogen-bonds, respectively. Therefore, we assume the energy difference between the $\mathbf{10c\text{-}s}$ and $\mathbf{10c\text{-}t}$ intermediates to be an approximate energy (11–12 kcal/mol) required for H–F bond formation between Selectfluor® (i.e., F-TEDA²+) and AgBF₄-coordinated hemiaminal (LOH). Notably, the open-shell singlet and triplet electronic states of the resulting adduct $\mathbf{11c}$ are very close in energy. As illustrated in Figure 8, overall, $\mathbf{8c\text{-}s} \to \mathbf{11c\text{-}s}$ is endergonic by $9.8/11.4 \text{ kcal/mol.}^{59}$

Interestingly, comparison of the $5c\text{-s} \to 5c\text{-t}$ and $10c\text{-s} \to 10c\text{-t}$ transitions show that the $5c\text{-s} \to 5c\text{-t}$ transition is a F-atom transfer from (F-TEDA)²⁺ to the Ag-center (or formal N–F oxidative addition) with an attendant electron transfer from substrate to the AgF-unit. It results in oxidation of both the Agcenter and substrate [form LH to the LH⁺]. In contrast, the $10c\text{-s} \to 10c\text{-t}$ transition is a simultaneous HF formation with only slight oxidation of the Ag-center.

Conversion of alkoxide intermediate **11c-s** to the final alkyl fluoride product (i.e., **LOF**, or **3**, see Figure 8) is a complex and multi-component process. It may occur through several pathways including (a) direct reaction with another equivalent of Selectfluor®:

{[(LO)-Ag]-(FH)-(TEDA)}²⁺ (11c-s) + (F-TEDA)²⁺
$$\rightarrow$$
 (Eq. 1)

and/or (b) directly by the HF by-product:

{[(LO)-Ag]-(FH)-(TEDA)}²⁺ (11c-s)
$$\rightarrow$$

(LOF) (3) + AgBF₄ + [H-TEDA]²⁺ (Eq. 2)

Since the reaction depicted in Eq. 1 is less exergonic than the reaction in Eq. 2 (by 0.1/20.1 kcal/mol vs 21.2/51.2 kcal/mol,

calculated relative to the complex **11c-s**), below we discuss Eq. 2 in detail, and include all calculated data for the reaction depicted in Eq. 1 in the Supporting Information (see Figures S7 and S8).

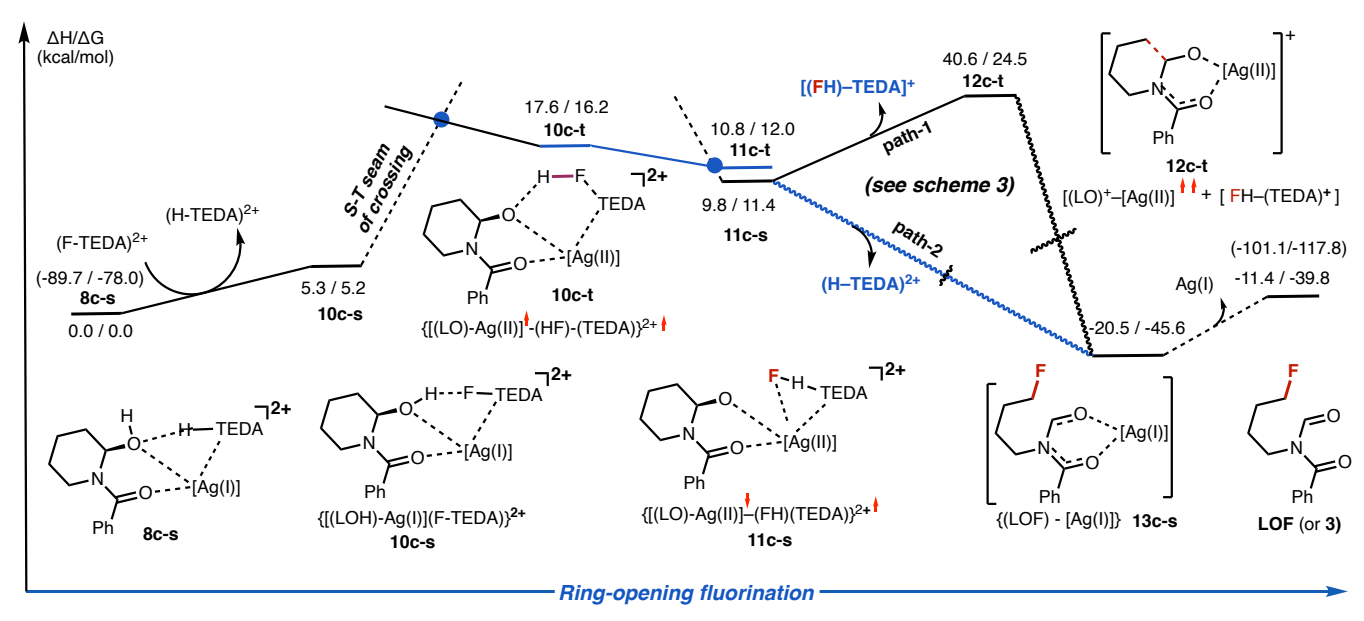


Figure 8. Energy profile of the reaction 8c-s + $[F-TEDA]^{2+} \rightarrow LOF$ (or 3) + Ag(I) + $[H-TEDA]^{2+}$. Energies given in parentheses are relative to the dissociation limit of [(LH)-Ag(I)], 4c-s, + $2[F-TEDA]^{2+}$.

The reaction depicted in Eq.2 can proceed through multiple pathways. One of them is a stepwise or dissociative-associative pathway (path-1), which is initiated by dissociation of [(FH)—TEDA]⁺, i.e. by the reaction:

{[(LO)-Ag]-(HF)-(TEDA)}²⁺ (11c-s)
$$\rightarrow$$
 [(LO)⁺-Ag] (12c-t) + [(FH)-TEDA]⁺ (Eq. 3)

(see Figure 8). Our calculations show that the dissociation of [(FH)-TEDA]⁺ from **11c-s** is endergonic by 30.8/13.1 kcal/mol and leads to formation of 12c-t and [(FH)-TEDA]+. Complex 12c-t, [(LO)*-Ag], where fragment (LO) bears almost one positive charge, has a triplet ground electronic state. Close analysis shows that most of the 1.70 |e| unpaired spin of the fragment (LO) is localized on the O-atoms (0.72 |e| and 0.37 |e| on the O^w and O_{amide}, respectively). The C2 and C3 centers have also acquired unpaired spins of 0.08 and 0.17 |e|, respectively. Importantly, the C2-C3 bond is elongated from 1.545 Å to 1.613Å, upon going from intermediate **11c-s** to **12c-t**. Thus, the oxidation of the (LO) unit of 11c-s is critical for the facile C2-C3 selective deconstructive fluorination of N-benzoylated cyclic amine 1. In the next step, [(FH)-TEDA]+ fragment coordinates to the C3-center of 12c-t and initiates the heterolytic cleavage of HF by the C3-center of 12c-t and TEDA+ monocation. The reaction 12c-t + [(FH)-TEDA] $^+ \rightarrow$ 13c-s + [H-TEDA] $^{2+}$ is calculated to be highly exergonic (by 61.1/70.1 kcal/mol). However, it is associated with an additional energy barrier at the triplet-singlet seam of crossing transition state. This transition state was not located because path-1 is energetically more uphill than path-2, which does not require dissociation of [(FH)-TEDA]+ from 11c-s, and has a lower associated energy barrier.

Scheme 3. Schematic Presentation of Elementary Reactions Involved in the Proposed Electron Transfer [From Alkoxide to (FH–TEDA)²⁺] Followed by Fluoride Trapping (by the C3-Center of Alkoxy Group) Mechanism of the 11c-s Transformation to [(LOF)–[Ag(I)].

Indeed, path-2 starts by translation of the [FH–TEDA] fragment to the vicinity of C3 followed by fluoride–C3 coupling and C3–C2 bond cleavage via the fluoride transfer mechanism. All our efforts to identify relevant intermediates and transition states, as well as their associated energies were unsuccessful. The scanning of the potential energy surface for F–C3 bond formation in **11c-s** led to the direct formation of [(**LOF**)–Ag(I)],

(13c-s), and [H-TEDA]²⁺ species with a low associated energy barrier (see Figure S10 in the Supporting Information). The overall reaction

{[(LO)-Ag]–(FH)–(TEDA)}²⁺ (11c-s)
$$\rightarrow$$

[(LOF)-Ag], (13c-s) +[H-TEDA]²⁺ (Eq. 4)

is calculated to be exergonic by 30.3/57.0 kcal/mol. The dissociation of Ag(I) from [(LOF)–Ag(I)] completes the formation of alkyl fluorinated product LOF (or 3), which requires only 5.8 kcal/mol free energy.

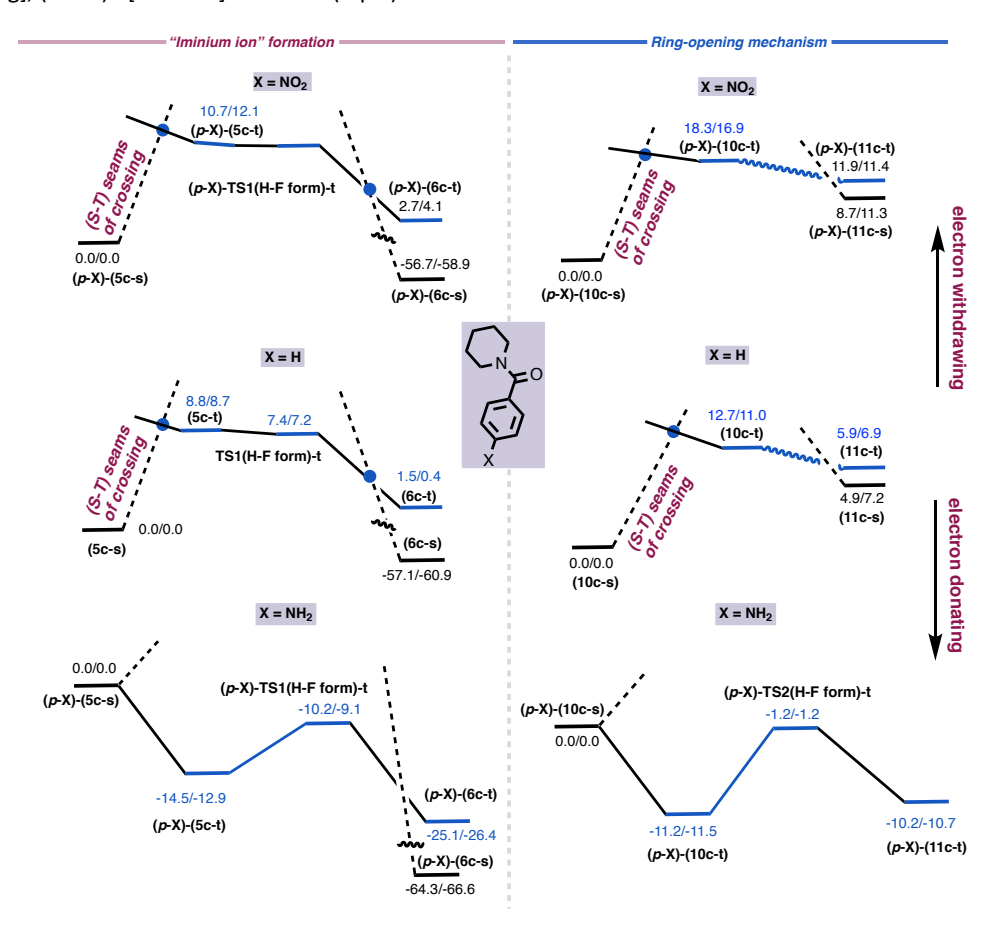


Figure 9. Energy surfaces (energies are given as $\Delta H/\Delta G$ in kcal/mol) of the iminium-ion formation and fluorination of hemiaminal via the ring-opening pathway for the unsubstituted (X =H) and para-X substituted N-protected cyclic amines (where X = NO₂ and NH₂).

On the basis of our computational findings, here, we propose that electron transfer followed by fluoride trapping by the nascent cation occurs (i.e., for the transformation of **11c-s** to **LOF**). This mechanistic scenario is consistent with that previously postulated by Sammis and co-workers.⁶⁰

The data presented thus far shows that both stages of the deconstructive fluorination of **LH** (or **1**), i.e., the hemiaminal formation (see Figure 1A–D) and the subsequent β -C–C cleavage and fluorination (Figure 1E, Path A), proceed via *TSR* mechanisms (triggered by the (S–T) seam of crossing). Since electron transfer from the substrate to the Ag-center is vital to the success of these reactions, the electronic properties of the *N*-benzoyl group of **LH** is expected to impact the nature of the reaction. Therefore, we extended our studies to substrates bearing *para* NO₂ and NH₂ substituents on the benzoyl group. The calculated structures of (*p*-X)-(5c-s), (*p*-X)-(5c-t), (*p*-X)-(10c-s), (*p*-X)-(10c-t), (*p*-X)-TS1(H-F form)-t, and (*p*-X)-TS1(H-F form)-t are given in the Supporting Information. Our calculations show that the reaction for (*p*-NO₂)–*N*-benzoylated cyclic amine will occur through a *TSR* mechanism, but barriers for both iminium

ion formation (i.e., analogous to **5c-s** \rightarrow **5c-t**) and the β -C–C cleavage/fluorination (i.e., analogous to **10c-s** \rightarrow **10c-t**) increase to 10.7/12.1 kcal/mol and 18.3/16.9 kcal/mol, respectively (see Figure 9). Thus, the AgBF₄-catalyzed fluorination of cyclic amines bearing an electron-withdrawing *para*-substituent on the *N*-benzoylated ring requires slightly higher energy barriers, but still proceeds via a *TSR* mechanism.

On the other hand, the presence of electron-donating groups on the *N*-benzoyl ring (for example, *para*-NH₂ substitution) not only changes the calculated energy barriers but also switches the mechanism of the reaction from *TSR* to the classical SET. As seen in Figure 9, for a *para*-NH₂ substituted *N*-protected cyclic amine [(*p*-NH₂)-LH], the triplet electronic state of (*p*-NH₂)-5c is more stable than its singlet electronic state by 14.5/12.9 kcal/mol. Therefore, upon the interaction of (*p*-NH₂)-(4c-s) with Selectfluor® a simultaneous spin decoupling occurs and electron transfer from (*p*-NH₂)-LH to (AgF)⁺ takes place via the classical *SET* mechanism. The hydrogen atom transfer/fluorine atom transfer coupling energy barrier at the

triplet transition state $[(p-NH_2)-TS1(H-F form)-t]$ is only 4.3/3.8 kcal/mol, relative to the triplet state in pre-reaction complex $(p-NH_2)-(5c-t)$.

Similarly, we found that the ground electronic state of (p-NH₂)-(10c) is the triplet state, which is 11.2/11.5 kcal/mol more stable than its singlet state. This results in a mechanism switch from TSR to SET in the C–C cleavage/fluorination of the hemiaminal via the ring-opening pathway. However, the calculated hydrogen-atom transfer and fluorine-atom transfer (HAT/FAT coupling) barrier for (p-NH₂)-TS2(H-F form)-t is 10.0/10.3 kcal/mol, which is only slightly lower than the 11.0-12.0 kcal/mol barrier assumed for the reaction of LH, where the benzoyl group does not bear any substituents.

On the basis of these computations, we conclude that deconstructive fluorination (via the β C–C cleavage pathway) of electron-poor N-benzoylated cyclic amines has a higher energy barrier and proceeds through a *two-state reactivity* mechanism. On the contrary, increased electron density on the N-benzoylated cyclic amine may not only slightly enhance its ring-opening fluorination by Selectfluor® but also introduces a mechanism switch to the broadly accepted SET mode.

C.2. Deformylative fluorination pathway (Path-B). We have also investigated the alternative pathway for C–C bond cleavage/fluorination that begins from the hemiaminal complex {[(LOH)-Ag](H–TEDA)}²⁺, 8c-s, (i.e., the "deformylative" fluorination pathway). This pathway is initiated by equilibration of the hemiaminal (LOH) to the corresponding aldehyde (Ald; Figure 10), which may occur either directly from complex 8c-s or following dissociation of (H–TEDA)²⁺ (i.e., in 9c-s; see Figures 7 and 10). While computations cannot unambiguously support either of these possibilities, they show that the conversion of (LOH) to linear aldehyde (I-Ald) is exergonic by 6.0 kcal/mol in the absence of other coordinating groups, and by 2.0 kcal/mol for the Ag-coordinated complex (i.e., complexes 9c-s and 14c-s, in Figure 10).

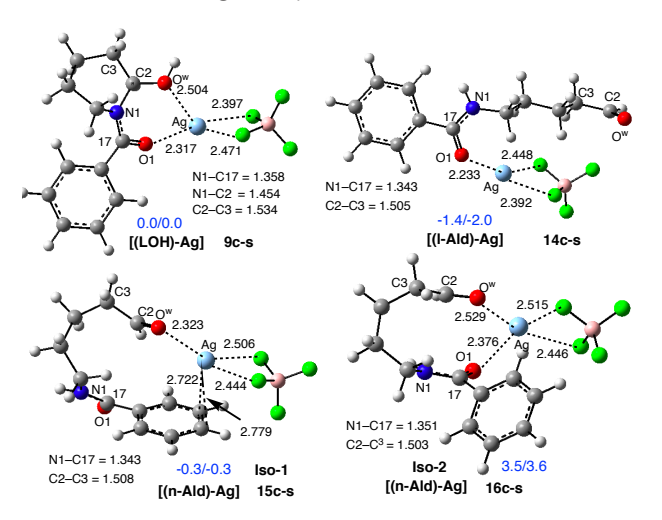


Figure 10. Calculated representative structures of hemiaminal-AgBF₄, **9c-s**, linear aldehyde-AgBF₄, **14c-s**, and two non-linear aldehyde-AgBF₄ complexes, **15c-s**, and **16c-s**, along with their key geometry parameters (distances are in Å), and relative energies given as $\Delta H/\Delta G$ in kcal/mol.

Because the interaction of [(LOH)-Ag] and [(Ald)-Ag] with Selectfluor® [i.e., (F-TEDA)²⁺] has minimal impact on the calculated geometries and energies, we began our analyses from the [(LOH)-Ag] and [(Ald)-Ag] complexes, which possess several isomers that are close in energy. A few of the energetically most favorable isomeric forms of these species are shown in Figure 10 (see also Figure S11 in the Supporting Information).

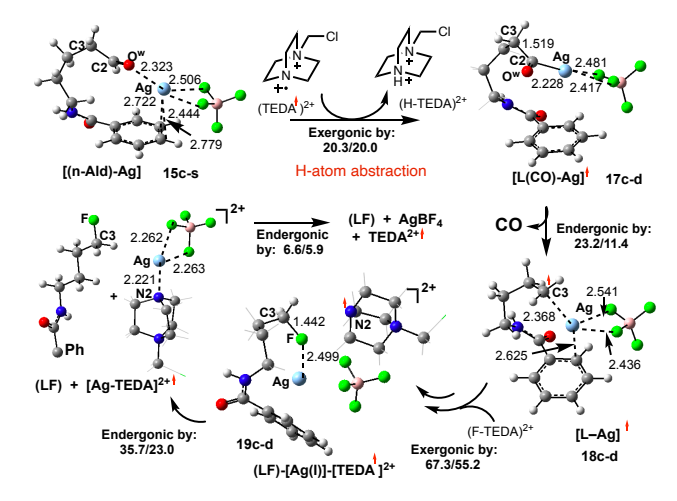


Figure 11. Calculated representative structures, along with their key geometry parameters (distances are in Å), for the proposed deformylative fluorination pathway. Energies (in kcal/mol) are provided relative to the pre-reaction complex as $\Delta H/\Delta G$.

As seen in Figure 10, in [(I-Ald)-Ag], 14c-s, the aldehyde group is coordinated to the Ag-center via the amide oxygen. In the lowest energy isomer of the non-linear aldehyde (n-Ald) and Ag-salt complex (i.e. 15c-s, iso-1), the Ag is coordinated to the oxygen atom (O^w) of the formyl group and Ph-ring of the benzoyl group. This isomer is 3.8–3.9 kcal/mol more stable than iso-2, i.e., complex 16c-s, where the Ag is coordinated to the aldehyde and amide carbonyl groups.

In principle, the formyl group could be oxidized to the corresponding carboxylic acid under the reaction conditions. The mechanism of the Ag(I)-catalyzed decarboxylative fluorination of aliphatic carboxylic acids by Selectfluor® has been previously investigated^{15,19} and established that these processes start with carboxylate coordination to the Ag(I)-center followed by oxidation of the resulting Ag-carboxylate by Selectfluor®:

RCOOH + Ag(I)
$$\rightarrow$$
 RCOO-Ag (Eq. 5)
RCOO-Ag + [F-TEDA]²⁺ \rightarrow
Ag(II)-OOCR + [TEDA]²⁺ + F⁻ (Eq. 6)

To the best of our knowledge, no detailed mechanistic studies on Ag-catalyzed deformylative fluorinations of hemiaminals by Selectfluor® have been reported in the literature. In our previous studies, attempts to monitor these processes only led to line broadening in the ¹H NMR and the appearance of carboxylic acid and aldehyde.^{8,9} Therefore, the direct deformylative pathway cannot be ruled out. In order to

investigate this possibility, we studied the Ag-catalyzed deformylative fluorination of aldehydes by Selectfluor® initiated from [(n-Ald)-Ag], 15c-s.

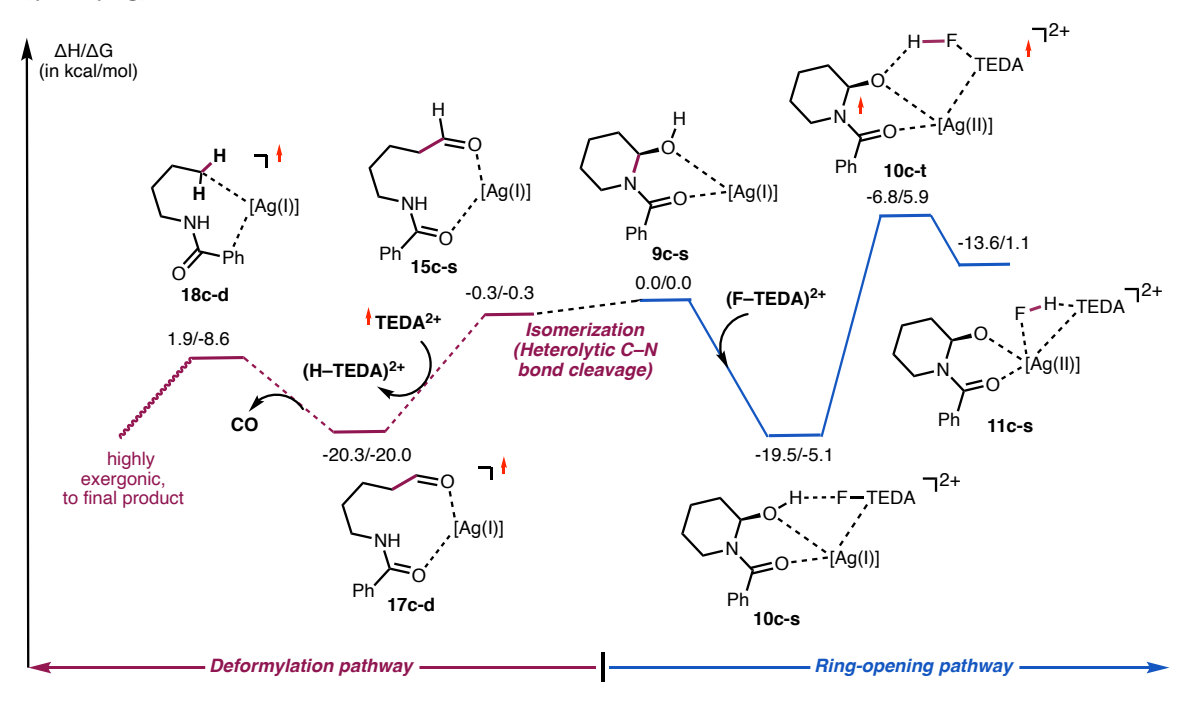


Figure 12. Comparison of the relative free energies of the initial steps of the ring-opening and deformylative fluorination of hemiaminal by Selectfluor®.

Our analyses indicate that deformylative fluorination of **15c-s** may proceed through several pathways (see Figure 12 and the Supporting Information for more details). We found that a pathway initiated by H-atom abstraction from **15c-s** by the previously generated radical dication TEDA²⁺ (see Figure 11) has the lowest associated energy barrier. The initial step of this pathway (Eq. 7):

[(n-Ald)-Ag], (15c-s) + TEDA^{2+*}
$$\rightarrow$$

[L(CO)-Ag], (17c-d) + [H-TEDA]²⁺ (Eq. 7)

occurs with almost no associated energy barrier and is exergonic by 20.3/20.0 kcal/mol. This result is in line with the findings of MacMillan and coworkers, 61 who have demonstrated a facile aldehydic H-atom abstraction by a quinuclidinium radical cation.

In the resulting complex (17c-d), the unpaired electron is localized on the CO-fragment (by 0.65 |e|), whereas the C3-center bears only 0.12 |e| unpaired spin. From this radical intermediate, loss of a CO molecule (that requires only 11.4 kcal/mol of free energy, see Figure 11), leads to [L-Ag], (18c-d). In intermediate 18c-d, one unpaired electron is distributed between the C3- and Ag-centers (0.71 |e| and 0.23 |e|, respectively) indicating that the C3 center is slightly oxidized and Ag(I)-center is slightly reduced (see Figure 11c in the Supporting Information for more details).

On the basis of the preceding discussion, it is anticipated that the C3-radical center of **18c-d** will undergo facile fluorination by another equivalent of Selectfluor®. A full scan of the reaction path (using the C3-[F-TEDA]²⁺ distance as a reaction

coordinate) demonstrates that this process has a very small associated energy barrier, and proceeds with the participation of the Ag-center. However, we were not able to locate any intermediates that possess a Ag–F bond (see also Figures S12 and S13 in the Supporting Information).²¹ The overall reaction

[L-Ag], (18c-d) + (F-TEDA)²⁺
$$\rightarrow$$
 [(LF)-Ag]-(TEDA)]²⁺, (19c-d) (Eq. 8)

is exergonic by 67.3/55.2 kcal/mol. On the basis of spin density analyses, we characterize **19c-d** as a (**LF**)-[Ag(I)]-[(TEDA)²⁺⁻], which possesses a dicationic TEDA radical. Dissociation of **LF** (i.e., **9**, in Figure 1) from **19c-d** is endergonic by 35.7/23.0 kcal/mol (see Figure 11).

In Figure 12 we compare the initial steps of the ring-opening (i.e., β -C–C cleavage) and deformylative fluorination of hemiaminal **9c-s** by Selectfluor®. Overall, the free energy barrier required for the ring-opening pathway, leading to the alkyl fluorinated product (**LOF**; or **3**), is 11.0 kcal/mol (using the energy span approach⁶²). The initial steps of the deformylative fluorination of the aldehyde intermediate, leading to **LF** (i.e., **9**), has an even smaller free energy barrier. Since we were not able to identify an energy barrier required for the hemiaminal \rightarrow aldehyde equilibration (which is expected to be small), here, we conclude that both pathways are feasible and preference of one over the other depends on the reaction conditions and the substrates that are employed.

Conclusions

Computational studies on the mechanism of the Ag(I)-mediated deconstructive fluorination of *N*-benzoylated piperidines (**LH**) described here provide evidence that:

- 1. The first-stage of the reaction, *i.e.*, the iminium ion formation, is, formally, a hydride abstraction event, and proceeds via: The subsequent formation of an iminium-ion intermediate, [L*-Ag]–HF–[TEDA]*, is, formally, a Ag(I)-mediated hydride abstraction event that occurs in two steps: (a) a formal oxidative addition (*OA*) of [F-TEDA]²⁺ to the Ag(I)-center that is attended by an electron transfer (*ET*) from substrate (LH) to the Ag-center (i.e., *OA+ET*, this process can also be referred to as a fluorine atom coupled electron transfer, FCET), and (b) H-atom abstraction from LH by the Ag-coordinated F-atom. The overall process involves lower-lying singlet and triplet electronic states of several intermediates, and is therefore, best *characterized as a two-state reactivity (TSR) event*. ²⁸⁻³⁵
- 2. The second-stage of the reaction is fluorination of the hemiaminal intermediate. This process may occur through either ring-opening or deformylative fluorination pathways. We found that a ring-opening fluorination (i.e., via $\beta\text{-C-C}$ cleavage/fluorination) is also a *two-state reactivity (TSR)* event. However, a competing deformylative fluorination is not a *TSR* event. Rather, it is initiated by a hemiaminal to aldehyde equilibration, followed by a formyl H-atom abstraction by a TEDA²⁺ radical dication, decarbonylation, and fluorination of the C3-radical center by another equivalent of Selectfluor®. Both fluorination pathways are feasible and preference for one over the other is subject to the reaction conditions and the substrates that are employed.
- 3. Facile oxidation of substrate is critical for both stages (i.e., the iminium ion formation and hemiaminal fluorination) of the *N*-benzoylated cyclic amine deconstructive fluorination. We have shown that ring-opening fluorination of the substrates bearing *para* electron-withdrawing substituents on the benzoyl group has a higher free energy barrier. On the contrary, substrates bearing electron-donating substituents on the *N*-benzoyl group enhance ring-opening fluorination by Selectfluor®.

The insights presented here are expected to aid in (a) identifying simpler, more efficient protocols for the deconstructive fluorination of N-acylated cyclic amines, (b) elucidating conditions that will effect deconstructive functionalization in aqueous solvent mixtures, and (c) lead to the widespread adoption of this method for late-stage skeletal diversification.

ASSOCIATED CONTENT

Supporting Information. Cartesian coordinates of all reported structures, and Figures S1–S13. This material is available free of charge via the Internet at http://pubs.acs.org.

AUTHOR INFORMATION

Corresponding Author

dmusaev@emory.edu

rsarpong@berkeley.edu

NOTES

The authors declare no competing financial interests.

ACKNOWLEDGMENT

This work was supported by the National Science Foundation under the CCI Center for Selective C–H Functionalization (CHE-1700982). R.S. is grateful to the NIGMS (R35 GM130345A) for support of the experimental work that was the basis for this computational study. The authors gratefully acknowledge the use of the resources of the Cherry Emerson Center for Scientific Computation at Emory University. J.B.R. thanks Bristol-Myers Squibb for a graduate fellowship.

REFERENCES

- 1) Cernak, T.; Dykstra, K. D.; Tyagarajan, S.; Vachal, P.; Krska, S. W. The Medicinal Chemist's Toolbox for Late-Stage Functionalization of Drug-Like Molecules. *Chem. Soc. Rev.* **2016**, *45*, 546–576.
- 2) Hartwig, J. F. Evolution of C–H Bond Functionalization from Methane to Methodology. *J. Am. Chem. Soc.* **2016**, *138*, 2–24.
- 3) Wang, B.; Perea, M. A.; Sarpong, R. Transition Metal-Mediated C–C Single Bond Cleavage: Making the Cut in Total Synthesis. *Angew. Chem., Int. Ed.* **2020**, *59*, 18898-18919.
- Murakami, M.; Ishida, N. Potential of Metal-Catalyzed C–C Single Bond Cleavage for Organic Synthesis. J. Am. Chem. Soc. 2016, 138, 13759–13769.
- O'Reilly, M. E.; Dutta, S.; Veige, A. S. β-Alkyl Elimination: Fundamental Principles and Some Applications. *Chem. Rev.* 2016, 116, 8105
 8145
- Souillart, L.; Cramer, N. Catalytic C–C Bond Activations via Oxidative Addition to Transition Metals. Chem. Rev. 2015, 115, 9410–9464.
- Roque, J. B.; Kuroda, Y.; Jurczyk, J.; Xu, L.-P.; Ham, J. S.; Göttemann, L. T.; Roberts, C.; Adpressa, D.; Saurí, J.; Joyce, L. A.; Musaev, D. G.; Yeung, C. S.; Sarpong, R. ACS Catal. 2020, 10, 2929–2941.
- 8) Roque, J. B.; Kuroda, Y.; Gottemann, L. T.; Sarpong, R. Deconstructive Fluorination of Cyclic Amines by Carbon-Carbon Cleavage. *Science* **2018**, *361*, 171-174.
- 9) Roque, J. B.; Kuroda, Y.; Gottemann, L. T.; Sarpong, R. Deconstructive Diversification of Cyclic Amines. *Nature* **2018**, *564*, 244-248.
- 10) Yu, C.; Shoaib, M. A.; Iqbal, N.; Kim, J. S.; Ha, H.-J.; Cho, E. J. Selective Ring-Opening of *N*-Alkyl Pyrrolidines with Chloroformates to 4-Chlorobutyl Carbamates. *J. Org. Chem.* **2017**, *82*, 6615–6620.
- 11) Feraldi-Xypolia, A.; Gomez Pardo, D.; Cossy, J. Ring Contraction of 3-Hydroxy-3 (trifluoromethyl)piperidines: Synthesis of 2-Substituted 2-(Trifluoromethyl)pyrrolidines. *Chem. Eur. J.* **2015**, *21*, 12876–12880
- 12) Wang, F.; He, Y.; Tian, M.; Zhang, X.; Fan, X. Synthesis of α-Formylated N-Heterocycles and Their 1,1-Diacetates from Inactivated Cyclic Amines Involving an Oxidative Ring Contraction, Org. Lett. 2018, 20, 864–867.
- 13) Huang, F.-Q.; Xie, J.; Sun, J.-G.; Wang, Y.-W.; Dong, X.; Qi, L. W.; Zhang, B. Regioselective Synthesis of Carbonyl-Containing Alkyl Chlorides via Silver-Catalyzed Ring-Opening Chlorination of Cycloalkanols. Org. Lett. 2016, 18, 684–6877.
- 14) Zhao, H.; Fan, X.; Zhu C. Silver-Catalyzed Ring-Opening Strategy for the Synthesis of β and γ -Florinated Ketons. *J. Am. Chem. Soc.* **2015**, *137*, 3490-3493.
- 15) Patel, N. R.; Flowers II, R. A. Mechanistic Study of Silver-Catalyzed Decarboxylative Fluorination. *J. Org. Chem.* **2015**, *80*, 5834-5841.
- 16) Michaudel, Q.; Thevenet, D.; Baran, P. S. Intermolecular Ritter-Type C–H Amination of Unactivated sp³-Carbons. *J. Am. Chem. Soc.* 2012, 134, 2547-2550.
- 17) Yayla, H. G.; Wang, H.; Tarantino, K. T.; Orbe, H. S.; Knowles, R. R. Catalytic Ring-Opening of Cyclic Alcohols Enabled by PCET

- Activation of Strong O-H Bonds. J. Am. Chem. Soc. 2016, 138, 10794-10797.
- 18) Pitts, C. R.; Bloom, S.; Woltornist, R.; Auvenshine, D. J.; Ryzhkov, L. R.; Siegler, M. A.; Lectka, T. Direct, Catalytic Monofluorination of sp³ Bonds: A Radical-Based Mechanism with Ionic Selectivity. *J. Am. Chem. Soc.* 2014, 136, 9780-9791.
- Yin, F.; Wang, Z.; Li, Z.; Li C. Silver-Catalyzed Decarboxylative Fluorination of Aliphatic Carboxylic Acids in Aqueous Solution. J. Am. Chem. Soc. 2012, 134, 10401-10404.
- Huang, X.; Hooker, J. M.; Groves, J. T. Targeted Fluorination with the Fluoride Ion by Manganese-Catalyzed Decarboxylation. *Angew. Chem. Int. Ed.* 2015, 54, 5241-5245.
- 21) Brandt, J. R.; Lee, E.; Boursalian, G. B.; Ritter, T. Mechanism of Electrophilic Fluorination with Pd(IV): Fluoride Capture and Subsequent Oxidative Fluoride Transfer. Chem Sci. 2014, 5, 169-179.
- 22) Zhu, Q.; Yang, P.; Chen, M.; Hu, J.; Yang, L. A Rapid Method to Aromatic Aminoalkyl Esters via the Catalyst-Free Difunctionalization of C–N Bonds. Synthesis 2018, 50, 2587–2594.
- 23) Romero-Ibañez, J.; Cruz-Gregorio, S.; Sandoval-Lira, J.; Hernández-Pérez, J. M.; Quintero, L.; Sartillo-Piscil, F. Transition-Metal-Free Deconstructive Lactamization of Piperidines. *Angew. Chem. Int. Ed.* **2019**, *58*, 8867–8871.
- 24) Zhang, Y.; Sun, S.; Su, Y.; Zhao, J.; Li, Y.-H.; Han, B.; Shi, F. Deconstructive di-functionalization of unstrained, benzo cyclic amines by C–N bond cleavage using a recyclable tungsten catalyst. *Org. Biomol. Chem.* 2019, 17, 4970–4974.
- Hua, A. M.; Mai, D. N.; Martinez, R.; Baxter, R. D. Radical C–H fluorination using unprotected amino acids as radical precursors. *Org. Lett.* 2017, 19, 2949-2952.
- 26) Ito, R.; Umezawa, N.; Higuchi, T. Unique Oxidation Reaction of Amides with Pyridine-N-oxide Catalyzed by Ruthenium Porphyrin: Direct Oxidative Conversion of N-Acyl-L-proline to N-Acyl-L-glutamate. J. Am. Chem. Soc. 2005, 127, 834-835.
- 27) Strictly speaking, this an electron transfer process. However, in the organic chemistry literature, such processes are referred to as SET events, analogous to the usage of these terms in electrocatalysis and photocatalysis. For consistency, here we also use the term single-electron transfer (SET).
- Schroder, D.; Shaik, S.; Schwarz, H. Two-state reactivity as a new concept in organometallic chemistry. Acc. Chem. Res. 2000, 33, 139-145.
- 29) de Visser, S. P.; Ogliaro, F.; Harris, N.; Shaik, S. Epoxidation of Ethene by Cytochrome P450: A Quantum Chemical Study. *J. Am. Chem. Soc.* **2001**, *123*, 3037-3047.
- 30) Klinker, E. J.; Shaik, S.; Hirao, H.; Que, Jr. L. Two-state reactivity model explains unusual kinetic isotope effect patterns in CH bond cleavage by non-heme oxoiron(IV) complexes. *Angew. Chem. Int.* Ed. 2009, 48, 1291-1297.
- 31) Musaev, D. G.; Morokuma, K. Ab Initio molecular orbital study of the electronic and geometrical structure of MCH₂+ and the reaction mechanism: MCH₂+ + H₂ → M⁺ + CH₄, (M = Co, Rh and Ir). *Isr. J. Chem.* **1993**, 33, 307-316.
- 32) Musaev, D. G.; Morokuma, K. Molecular orbital study of the mechanism of Sc⁺ with methane. Comparison of the reactivity of early and late first-row transition metal cations and their carbene complexes. J. Phys. Chem. 1996, 100, 11600-11609.
- Musaev, D. G.; Morokuma, K. Potential energy surface of transition metal catalyzed chemical reactions. Adv. Chem. Phys. 1996, 61-128.
- 34) Musaev, D. G.; Morokuma, K.; Koga, N.; Nguyen K. A.; Gordon. M. S.; Cundari, T. R. An Ab Initio study of the molecular and electronic structure of CoCH₂⁺ and the reaction mechanism: CoCH₂⁺ + H₂. J. Phys. Chem. 1993, 97, 11435-11444.
- 35) Musaev, D. G.; Koga, N.; Morokuma, K. Ab Initio molecular orbital study of the electronic and geometrical structure of RhCH₂+ and the reaction mechanism: RhCH₂+ + H₂ → Rh+ + CH₄. *J. Phys. Chem.* **1993**, *97*, 4064-4075.

- 36) Frisch, M. J.; Trucks, G. W.; Schlegel, H. B.; Scuseria, G. E.; Robb, M. A.; Cheeseman, J. R.; Scalmani, G.; Barone, V.; Petersson, G. A.; Nakatsuji, H.; Li, X.; Caricato, M.; Marenich, A. V.; Bloino, J.; Janesko, B. G.; Gomperts, R.; Mennucci, B.; Hratchian, H. P.; Ortiz, J. V.; Izmaylov, A. F.; Sonnenberg, J. L.; Williams-Young, D.; Ding, F.; Lipparini, F.; Egidi, F.; Goings, J.; Peng, B.; Petrone, A.; Henderson, T.; Ranasinghe, D.; Zakrzewski, V. G.; Gao, J.; Rega, N.; Zheng, G.; Liang, W.; Hada, M.; Ehara, M.; Toyota, K.; Fukuda, R.; Hasegawa, J.; Ishida, M.; Nakajima, T.; Honda, Y.; Kitao, O.; Nakai, H.; Vreven, T.; Throssell, K.; Montgomery, J. A., Jr.; Peralta, J. E.; Ogliaro, F.; Bearpark, M. J.; Heyd, J. J.; Brothers, E. N.; Kudin, K. N.; Staroverov, V. N.; Keith, T. A.; Kobayashi, R.; Normand, J.; Raghavachari, K.; Rendell, A. P.; Burant, J. C.; Iyengar, S. S.; Tomasi, J.; Cossi, M.; Millam, J. M.; Klene, M.; Adamo, C.; Cammi, R.; Ochterski, J. W.; Martin, R. L.; Morokuma, K.; Farkas, O.; Foresman, J. B.; Fox, D. J., Gaussian 16, Revision C.01, Gaussian, Inc., Wallingford CT, 2019.
- 37) Hay, P. J.; Wadt, W. R. Ab Initio Effective Core Potentials for Molecular Calculations. Potentials for the Transition Metal Atoms Sc to Hg. J. Chem. Phys. 1985, 82, 270-283.
- Hay, P. J.; Wadt, W. R. Ab Initio Effective Core Potentials for Molecular Calculations. Potentials for K to Au Including the Outermost Core Orbitals. J. Chem. Phys. 1985, 82, 299-310.
- 39) Wadt, W. R.; Hay, P. J. Ab Initio Effective Core Potentials for Molecular Calculations. Potentials for Main Group Elements Na to Bi. *J. Chem. Phys.* **1985**, *82*, 284-298.
- Becke, A. D. Density-Functional Exchange-Energy Approximation with Correct Asymptotic Behavior. *Phys. Rev. A* 1988, 38, 3098-3100.
- Lee, C.; Yang, W.; Parr, R. G. Development of The Colle-Salvetti Correlation-Energy Formula into a Functional of the Electron Density. *Phys. Rev. B* 1988, 37, 785-789.
- 42) Becke, A. D. A New Mixing of Hartree–Fock and Local Density-Functional Theories. *J. Chem. Phys.* **1993**, *98*, 1372-1377.
- 43) Grimme, S.; Antony, J.; Ehrlich, S.; Krieg, H. A Consistent and Accurate Ab Initio Parametrization of Density Functional Dispersion Correction (DFT-D) for the 94 Elements H-Pu. *J. Chem. Phys.* **2010**, *132*, 154104-154122.
- Becke, A. D.; Johnson, E. R. A Density-Functional Model of the Dispersion Interaction. J. Chem. Phys. 2005, 123, 154101-154106.
- 45) Becke, A. D.; Johnson, E. R. Exchange-Hole Dipole Moment and the Dispersion Interaction. *J. Chem. Phys.* **2005**, *122*, 154104-154109
- 46) Johnson, E. R.; Becke, A. D. A Post-Hartree-Fock Model of Intermolecular Interactions: Inclusion of Higher-Order Corrections. J. Chem. Phys. 2006, 124, 174104-174112.
- 47) Barone, V.; Cossi, M. Quantum Calculation of Molecular Energies and Energy Gradients in Solution by a Conductor Solvent Model. J. Phys. Chem. A 1998, 102, 1995-2001.
- Cossi, M.; Rega, N.; Scalmani, G.; Barone, V. Energies, Structures, and Electronic Properties of Molecules in Solution with the C-PCM Solvation Model. *J. Comput. Chem.* 2003, 24, 669-681.
- 49) A New Basis Set Exchange: An Open, Up-to-date Resource for the Molecular Sciences Community Benjamin P. Pritchard, Doaa Altarawy, Brett Didier, Tara D. Gibson, and Theresa L. Windus J. Chem. Inf. Model. 2019, 59(11), 4814-4820
- Chai, J.-D.; Head-Gordon, M. Long-range Corrected Hybrid Density Functionals with Damped Atom-Atom Dispersion Corrections. Phys. Chem. Chem. Phys. 2008, 10, 6615-6620;
- 51) The triplet electronic state of this adduct, i.e., **4c-t** (see the Supporting Information), is 77.3/74.3 kcal/mol higher in energy, where unpaired α -spins are mostly located in **LH**.
- 52) Yarkony, D. Diabolical Conical Intersections. *Rev. Modern Physics* **1996**, *68*, 985–1013.
- 53) Since **LH** has a lower ionization potential as compared to AgBF₄, **LH** is oxidized more readily than the Ag(I)-salt upon interaction of with Selectfluor®. Consistently, in **5c-s**, a (S-T) transition, mostly, engages an intra-substrate electron transfer process.

- 54) Font, M.; Acuna-Pares, F.; Parella, T.; Serra, J.; Luis, J. M.; Lloret-Fillol, J.; Costas, M.; Ribas, X. Nat. Commun. **2014**, *5*, 4373.
- 55) Ajitha, M. J.; Pary, F.; Nelson, T. L.; Musaev, D. G. Unveiling the role of base and additive in the Ullmann-type of arene-aryl C–C coupling reaction. ACS Catalysis 2018, 8, 4829-4837.
- 56) In this TS, as compared to the pre-reaction complex **5c-t**, the nascent H1–F bond is shortened to 1.502Å from 1.943Å, whereas the C2–H1 and Ag–F bonds are elongated to 1.177 and 2.100Å from 1.089 and 2.040Å, respectively. Of note is the shortening of the N1–C2 and N1–C17 bond distances, which is consistent with the changes in spin densities on the N1- and C2-centers. Indeed, the unpaired spin density at N1 is reduced from 0.67 to 0.50 |e|, whereas the spin density at C2 has increased from 0.12 to 0.24 |e| upon going from **5c-t** to **TS1(H-F form)-t**.
- Beatty, J. W.; Stephenson, C. R. J. Amine Functionalization via Oxidative Photoredox Catalysis: Methodology Development and Complex Molecule Synthesis. Acc. Chem. Res. 2015, 48, 1474–1484.
- 58) As illustrated in Figure 6, for complex **8c-s**, H-TEDA is hydrogen bonded to the hemiaminal (**LOH**) with an O^w--H(TEDA) bond length of 1.659Å. Also, the Ag(I) center is coordinated to the amide oxygen

- of **LOH** with a Ag–O bond length = 2.219Å. Importantly, in going from **7c-s** to **8c-s**, the N1–C17 bond is shortened from 1.478Å to 1.360 Å, whereas the N1–C2 bond is elongated from 1.297 Å to 1.462Å. These geometry changes are consistent with hemiaminal formation.
- 59) The +2 total charge of **11c** is mostly localized on TEDA unit (which has a +1.77 and 1.75 |e| charge in its singlet and triplet states, respectively). Furthermore, the calculated H–TEDA bond distance is 1.073 and 1.101 Å, in **11c-s** and **11c-t**, respectively.
- 60) Rueda-Becerril, M.; Sazepin, C. C.; Leung, J. C. T.; Okbinoglu, T.; Kennepohl, P.; Paquin, J.-F.; Sammis, G. M. Fluorine Transfer to Alkyl Radicals. J. Am. Chem. Soc. 2012, 134, 4026–4029.
- 61) Zhang, X.; MacMillan, D. W. C. Direct Aldehyde C-H Arylation and Alkylation via the Combination of Nickel, Hydrogen Atom Transfer, and Photoredox Catalysis. J. Am. Chem. Soc., 2017, 139, 11353-11356.
- 62) Kozuch, S.; Shaik, S. How to conceptualize catalytic cycles? The energetic span model. *Acc. Chem. Res.* **2011**, *44*, 101-110.

Insert Table of Contents artwork here

Ag(I)-Mediated Deconstructive Fluorination of Cyclic Amines